The Journal of Supercritical Fluids 133 (2018) 278–290

Contents lists available at ScienceDirect

The Journal of Supercritical Fluids

journal homepage: www.elsevier.com/locate/supflu

Carvone-loaded LDPE films for active packaging: Effect of supercritical CO_2-assisted impregnation on loading, mechanical and transport properties of the films

María L. Goñi[a,b], Nicolás A. Gañán[a,b,*], Raquel E. Martini[a,b], Alfonsina E. Andreatta[c]

[a] IPQA, UNC, CONICET, Av. Vélez Sarsfield 1611, X5016GCA, Córdoba, Argentina
[b] Universidad Nacional de Córdoba, Facultad de Ciencias Exactas, Físicas y Naturales, Instituto de Ciencia y Tecnología de los Alimentos – ICTA. Av. Vélez Sarsfield 1611, Córdoba, Argentina
[c] UTN – Facultad Regional San Francisco, CONICET. Av. de la Universidad 501, San Francisco, Córdoba, Argentina

GRAPHICAL ABSTRACT

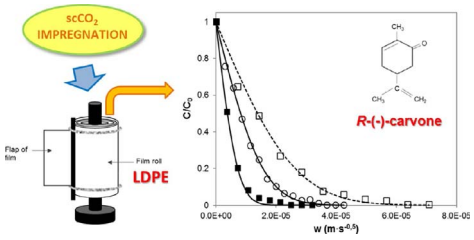

ARTICLE INFO

Keywords:
Supercritical fluid impregnation
R-(−)-carvone
LDPE
Active packaging
Diffusion coefficient

ABSTRACT

In this work, low density polyethylene (LDPE) films were loaded by $scCO_2$-assisted impregnation with *R*-(−)-carvone, the main component of *M. spicata* and *A. polystachya* essential oils with antimicrobial and insecticidal activity. Impregnation runs were performed in a lab-scale high-pressure cell, and the effect of CO_2 density (240–700 kg m^{-3}) and temperature (35–60 °C) on impregnation yield was evaluated. Impregnation yields of 2.0–4.8% (w/w) were obtained, achieving higher values at low CO_2 density. Thermal and mechanical properties of the films, before and after impregnation, were also investigated. The diffusion coefficient of carvone in $scCO_2$-swollen films was estimated by impregnating film rolls and modeling the concentration profile through the roll thickness using an analytical solution of second Fick's law. Release profiles into air were determined, allowing to estimate diffusivity values in non-swollen films at ambient conditions.

1. Introduction

Supercritical CO_2 ($scCO_2$) assisted impregnation of polymeric films has been proposed and studied by several authors as a suitable technology for producing active materials for food packaging applications. In this way, a great variety of polymeric materials (petroleum-based as well as natural biopolymers) have been impregnated with antioxidant [1,2], antimicrobial [3–5] and insecticidal agents [6–8] using $scCO_2$ as solvent and swelling agent. In addition to the well-known advantages of $scCO_2$ as an eco-friendly solvent [9–12] and the high solubility of many natural active compounds even at mild conditions, $scCO_2$-assisted impregnation is based on the ability of $scCO_2$ to absorb in many polymeric matrices and swell them, increasing the system free volume and the mobility of the polymer chains, enhancing internal diffusivity in several orders of magnitude [9]. Under this state, the solute molecules dissolved in the supercritical fluid phase can penetrate more easily into the

* Corresponding author at: IPQA, Universidad Nacional de Córdoba, CONICET, Av. Vélez Sarsfield 1611, X5016GCA, Córdoba, Argentina.
E-mail address: nganan@plapiqui.edu.ar (N.A. Gañán).

http://dx.doi.org/10.1016/j.supflu.2017.10.019
Received 27 July 2017; Received in revised form 25 October 2017; Accepted 25 October 2017
Available online 28 October 2017
0896-8446/ © 2017 Elsevier B.V. All rights reserved.

polymer network, where specific interactions may occur. After some contact time, which can lead to polymer saturation, the system is depressurized, CO_2 molecules are rapidly desorbed from the polymer and, due to the drastic decrease in solubility and diffusivity, solute molecules are retained into the matrix to a great extent. As a result, polymers are generally impregnated more deeply and faster than when liquid solvents are used.

On the other hand, in the last decades the activity of several botanic compounds has been studied and proposed for their use as active substances in replacement of synthetic additives in order to improve food safety and extend its shelf life. Simultaneously, due to the increasing consumer demands for minimally processed and preservative-free products, food industries perceive active and intelligent packaging as a promising technology for food preservation. Furthermore, this interest has been encouraged by the publication of new regulations concerning the use of these active materials in food contact applications. Consequently, the incorporation of EOs in plastic films to avoid food spoilage is nowadays considered an attractive option for packaging manufacturers and demanding consumers [13–17].

In this work, the incorporation of carvone (2-methyl-5-(prop-1-en-2-yl)cyclohex-2-en-1-one) into low density polyethylene (LDPE) films using $scCO_2$-assisted impregnation technology is investigated. Carvone, whose chemical structure is shown in Fig. 1, is the main component of several essential oils (EOs). This compound has been used for decades in the food industry as a flavoring agent, but nowadays it plays a new role due to its antimicrobial and insecticidal activity [16]. It is an optically active monoterpene, being a very effective bioinsectide as well as antimicrobial agent, presenting both antibacterial and antifungal activities. Moreover, many *in vitro* evaluations have demonstrated the antimicrobial properties of both optical isomers [16–18]. In particular, *R*-(−)-carvone has been proved to be very effective against storage diseases of potatoes like silver scurf and dry rot, caused by *Helminthosporium solanii* and *Fusarium sulfureum* [16]. The insecticidal activity of *R*-(−)-carvone and essential oils rich in this compound has also been reported by several authors. For instance, spearmint EO and pure *R*-(−)-carvone have proved to be highly toxic against adults moths [19] and stored product beetles [20–22].

Several authors have studied and reported the incorporation of active EOs (and their purified components) as well as other extracts from plants into a wide spectrum of both bio- and petroleum-based polymeric matrices commonly used for food packaging by different methodologies [23]. Nevertheless, active packaging systems are mostly based on polyolefin-based films −due to their good technological properties (mechanical, barrier, optical and thermal)– combined with antimicrobial or antioxidant additives [24,25].

Several techniques are conventionally used at industrial scale for incorporating active substances or additives into polymers. Some of them imply the risk of thermal decomposition of sensitive organic compounds due to they operate above the polymer melting temperature, such as hot melt extrusion or casting techniques. In other processes organic liquid solvents are used which must be removed afterwards in order to meet the rigorous regulations concerning materials for food, biomedical and pharmaceutical applications [26]. $ScCO_2$-assisted impregnation overcomes both limitations, allowing to operate at mild temperature conditions and without liquid solvents, and it has been proven to be very effective for developing active packaging materials exhibiting the same kind of activity as the pure active compounds [1,3,4,27–29]. Nevertheless, to the best of our knowledge, the incorporation of carvone in LDPE films using $scCO_2$-assisted impregnation has not been yet reported in the literature.

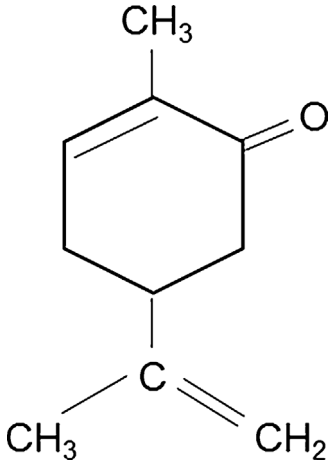

Fig. 1. Chemical structure of *R*-(–)-carvone.

Although in most studies single films are impregnated (generally until saturation), industrially it is more convenient to deal with film rolls. In this sense, the few studies that have undertaken pilot or industrial scale research −which are related to $scCO_2$-assisted dying of textile polymers [30,31] have included the impregnation of entire rolls of film. The design and optimization of such processes require some knowledge of the diffusion coefficient of the loaded substance into the swollen polymer at supercritical conditions, as well as the saturation (thermodynamic) loading limit.

Moreover, it is also important to assess the possible effects of the supercritical impregnation treatment on the thermal and mechanical properties of the material. Morphological changes −such as the modification in crystallinity degree, or the rearrangement of crystalline domains–may be induced by $scCO_2$ sorption and the incorporation of additives, which can in turn affect the mechanical behavior, in terms of strength, ductility and elasticity. These properties represent relevant parameters for evaluating an application, as they indicate the ability of the material to maintain integrity under the stress conditions related to processing, handling and storage [3,32,33].

Based on these facts, the objectives of this work are: (a) to determine the impregnation yield of *R*-(–)-carvone in LDPE films at different temperature and pressure conditions; (b) to determine the diffusion coefficient of *R*-(–)-carvone in $scCO_2$-swollen LDPE at different operation conditions, using a film-roll method [34]; (c) to evaluate the thermal and mechanical properties of the obtained films and detect possible modifications due to the impregnation treatment; (d) to study the release kinetics of *R*-(–)-carvone from the impregnated films, determining its diffusion coefficient under ambient conditions.

2. Materials and methods

2.1. Materials

Commercial films of low density polyethylene (LDPE, density: 896 kg m^{-3}, thickness: 30 ± 1 μm) used as polymeric matrix in the impregnation tests, were kindly provided by Converflex (ARCOR Group, Córdoba, Argentina).

R-(–)-carvone (purity: 98%; bp: 227–230 °C; MW: 150.22 g/mol) was purchased from Sigma-Aldrich (Steinheim, Germany) and industrial extra-dry carbon dioxide (water content ≤ 10 ppm v/v), used as impregnation solvent, from Linde (Argentina).

Ethanol (96% v/v, food grade, Porta, Argentina) was used as solvent in the characterization tests.

2.2. Supercritical impregnation experiments

$ScCO_2$–assisted impregnation runs were carried out in a lab-scale batch system described in a previous work [26] and schematically shown in Fig. 2. In brief, each impregnation run was performed in a high-pressure cell (a stainless-steel vessel of 50 cm^3 of internal volume), under constant pressure, temperature and agitation conditions for a period of time, after which the CO_2 was released at constant depressurization rate using a micrometering valve.

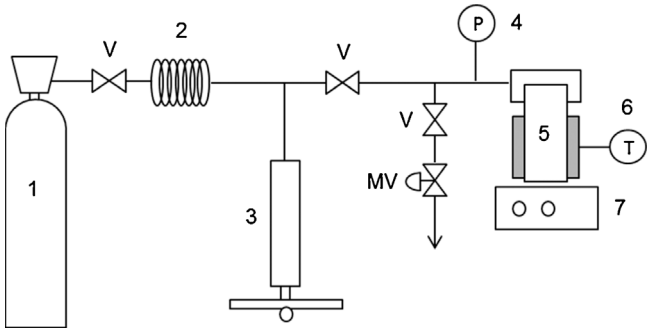

Fig. 2. High-pressure impregnation system. 1: CO_2 reservoir; 2: cooling coil; 3: pressure generator; 4: manometer; 5: impregnation cell; 6: temperature controller; 7: magnetic stirrer; V: valves; MV: micrometering valve.

In this work, impregnation runs were performed at two temperature levels (35 and 60 °C) and four CO_2 density levels (~240-700 kg·m^{-3}), while depressurization was performed at a constant rate of 0.6 MPa·min^{-1} for all runs. CO_2 density was controlled by setting the system pressure at proper values. For this purpose, pure CO_2 data from NIST were used [35]. The experimental conditions for all runs are shown in Table 1. The initial concentration of carvone in the fluid phase was fixed and selected in order to operate under single phase conditions, i.e., below the solubility value at each temperature and pressure condition. The corresponding amounts of carvone loaded into the cell in each experiment were calculated taking into account the cell volume and the corresponding CO_2 density. The determination of the carvone solubility in CO_2 is explained in Section 2.3.

In each run, three films (approx. 10 cm^2 each) were placed into the cell using a metal-mesh support, the corresponding amount of carvone was loaded and the cell immediately closed. The support allowed to maintain the films separated from each other and in a vertical position, allowing the diffusion through both sides of the films as well as minimizing the precipitation of carvone droplets onto the film surfaces during the depressurization step. Afterwards, CO_2 was delivered to the cell until the desired pressure was achieved (corresponding to the specified temperature and density conditions), and the system was kept at constant pressure and temperature for 2 h, after which the CO_2 was released from the system at a constant depressurization rate (0.6 MPa·min^{-1}). Preliminary tests were conducted at different times (t = 2–4 h) in order to check whether the saturation of the films with carvone occurred at t = 2 h.

The films were removed from the cell and gently dried with tissue paper in order to remove any residual amount of carvone from the surface. The mass of carvone loaded into the films was calculated gravimetrically by measuring the mass gain of the films after the assay in a precision balance (± 0.0001 g). Then, the impregnation yield (Y%) was defined as follows (Eq. (1)):

$$Y\% = \frac{m_f - m_0}{m_0} \times 100 \quad (1)$$

where m_o and m_f are the original and the final mass of the film, before and after impregnation, respectively.

Table 1
Experimental conditions for the impregnation of LDPE films with *R*-(–)-carvone. Depressurization rate = 0.6 MPa·min^{-1} and time = 2 h for all runs.

Run no.	Temperature (°C)	Pressure (MPa)	CO_2 density (kg m^{-3})
1	35	7.6	288.4
2	60	9.1	240.3
3	35	7.9	365.5
4	60	11.5	395.8
5	35	8.1	490.8
6	60	13.4	529.6
7	35	9.7	700.7

Preliminary tests were performed in order to ensure that the film mass is not affected by the pressurization-depressurization process (e.g., due to the extraction of additives) as well as to confirm that CO_2 desorption from the films is complete within few minutes after depressurization [7]. These tests were carried out by treating LDPE films with pure scCO_2 at the operation conditions and weighing them after depressurization. It was verified that the films recovered their original weight within 2 min, indicating a fast desorption of CO_2. In the same way, it was verified in release experiments from carvone-loaded films that the mass loss due to carvone desorption was in the order of 1–2% in the same period.

The gravimetric determination was validated by comparison with UV spectrophotometric analysis of selected samples. Film samples of known mass were placed in flasks containing ethanol under vigorous agitation during 1 h, in order to extract the impregnated carvone. Two extraction steps were required in order to exhaust the film samples. The concentration of carvone in the ethanolic solution was then determined by measuring absorbance at 236 nm in a UV–vis spectrophotometer (Lambda 25, Perkin Elmer, USA). For that purpose, a calibration curve was prepared using different concentrations of carvone in ethanol ranging from 0.002 to 0.040 mg·ml^{-1}. The absorbance at 236 nm of this set of solutions was acquired, and the relationship between the concentration of carvone and the absorbance was adjusted with a linear function. The calibration curve was performed by duplicate. The extraction of carvone was considered complete after obtaining at least two carvone-free extracts. Furthermore, direct UV analysis of the exhausted films was performed immediately afterwards, using a neat LDPE film as reference, confirming the absence of the carvone absorption peak in the spectrum.

2.3. Estimation of carvone solubility in scCO_2

In order to perform the impregnation tests at homogeneous conditions in the fluid phase, as previosuly mentioned, the concentration of carvone was set below its solubility value at each condition. For that purpose, the solubility behavior of carvone in scCO_2 at 35 °C and 60 °C was estimated by predictive calculations using the Group Contribution Equation of State (GC-EOS) [36], over the experimental range. The model equations and the parameters (pure group, binary interaction and binary non-randomness parameters) used in the calculations, as well as the group structures, are reported in Appendix A. With this set of equations, the solubility was calculated from the equilibrium mole fraction of carvone in the CO_2 phase by solving multiphasic P,T-flashes with the subroutine GCTHREE [37].

GC-EOS calculations were previously validated by comparison with experimental data reported in the literature at 39 and 49 °C within a pressure range of 6–10 MPa [38,39]. The model deviation was estimated as the average absolute relative deviation (AARD%) at each temperature, defined as (Eq. (2)):

$$AARD\% = \frac{1}{NP}\sum_{i=1}^{NP}\frac{|y_{calc,i} - y_{exp,i}|}{y_{exp,i}} \times 100 \quad (2)$$

where y_{calc} and y_{exp} are the calculated and experimental solubility values (in mole fraction) and NP is the number of experimental points.

2.4. Fourier transformed infra-red spectrometric analysis (FTIR)

Impregnated film samples were analyzed by Fourier transformed infrared (FTIR) spectrometry in order to confirm the incorporation of carvone. Absorbance spectra were obtained in an infrared imaging microscope (Nicolet iN10 Mx, Thermo Fisher Scientific, USA), with a resolution of 2 cm^{-1}, in a wavenumber range of 400–4000 cm^{-1} with 16 scans, at room temperature. Spectra of pure carvone, neat LDPE film and impregnated film samples were acquired and compared in order to

identify characteristic absorbance bands. Background spectra were acquired before each test for air humidity and carbon dioxide correction.

2.5. Differential scanning calorimetry (DSC)

Thermal properties were evaluated in a Discovery DSC equipment (TA Instruments, USA). Thermograms were obtained directly on film samples heating from 25 °C to 180 °C and cooling from 180 °C to 25 °C, both at a rate of 10 °C min^{-1}. Analysis was performed on neat polymer films as well as impregnated samples in order to evaluate the variation of the properties during high-pressure treatment (with and without carvone). For this reason, as the polymer thermal history should not be removed, only the first heating cycle was considered. Melting temperatures and enthalpies were recorded, and the crystallinity degree was calculated taking into account all melting peaks in the thermograms, by comparison with the melting enthalpy of pure crystalline LDPE ($\Delta H_m = 288$ J/g).

2.6. Mechanical properties

In order to determine the impact of the high pressure treatment and the incorporation of carvone on the mechanical properties of the films, tensile strength tests were performed on carvone-impregnated, $scCO_2$-pressurized and neat polymer film samples, using a universal testing machine (Instron, USA). Rectangular probes (100 × 10 mm) were used in all cases, with an initial grip separation of 70 mm. Tests were conducted under a constant cross-head speed of 100 mm min^{-1} until break. Young modulus, yield strength, tensile strength and elongation at break were recorded along each test and reported as mean value ± standard deviation of at least 6 replicates.

2.7. Diffusion coefficient estimation under impregnation conditions

The mass transfer kinetics of carvone in LDPE films under $scCO_2$ conditions was investigated by studying the effect of temperature and CO_2 density on the diffusion coefficients of this compound in the films. For that purpose, the "film roll method" reported by Sicardi et al. [34] was used, with some modifications. For all the experiments, the film roll was prepared as follows: First, polymer film strips of 2–5 m length (depending on the experiment) and 2 cm wide were wrapped tightly around a glass tube of 0.6 cm diameter forming a roll, which was held together by a capillary glass rod pressed against it by two Teflon© threads, keeping a flap of film (2 cm long) separated from the roll in order to be in contact with the $scCO_2$ by both sides. A graphical representation of the film roll is shown in Fig. 3. These precautions were taken in order to avoid direct contact of the inner layers of the roll with the fluid phase and ensure that the mass transfer of carvone is by diffusion from outer to inner layer, as in a continuous medium [34]. The roll was then placed into the high-pressure cell previously described in Section 2.2, and impregnation was conducted for a certain period of time, which varied in each experiment and was in the range 40–60 min. After depressurization, the films were unrolled and cut in pieces of approx. 1.5 cm × 1.5 cm, each one corresponding to a film layer. These pieces were cut from the center of the strip, leaving apart de edges (which might be exposed to direct contact with $scCO_2$ due to small imperfections of the rolls). The amount of carvone incorporated in each film sample was determined by extraction with ethanol and UV spectrophotometric analysis following the same procedure described in Section 2.2. The exhausted films were allowed to dry until constant weight, which was assumed to be equal to the original (carvone-free) weight. In this way, the concentration profile of carvone over the film roll thickness was determined for each experiment.

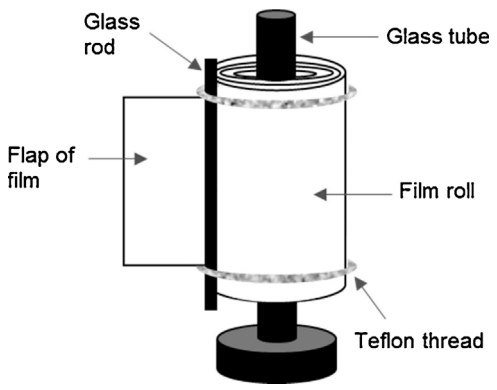

Fig. 3. Diagram of film roll used for diffusion experiments.

From these data, the diffusion coefficient of carvone in the $scCO_2$-swollen LDPE films was estimated by fitting a mass transfer model based on the second Fick's law for non-steady diffusion, as proposed by Crank [40]. The following hypothesis are assumed: (a) the diffusion process can be described by Fick's laws; (b) the film roll can be described as a unidimensional slab, as its thickness is small compared to its total diameter; (c) $scCO_2$ sorption is faster than carvone diffusion, and therefore the polymer roll is considered to be completely swollen when impregnation begins; (d) the concentration of carvone in the film at the fluid-polymer interphase (C_0) is constant, as the $scCO_2$ phase is saturated throughout the experiment; (e) the diffusion coefficient of carvone under supercritical impregnation conditions (D_{SC}) is constant, which can be assumed due to its low concentration in the film. Under these assumptions, an analytical solution of the second Fick's law is given by Eq. (3):

$$\frac{C}{C_0} = erfc\left(\frac{w}{D_{SC}^{1/2}}\right) \tag{3}$$

where C is the concentration of carvone in each layer, and the variable w is defined as:

$$w = \frac{x}{2t^{1/2}} \tag{4}$$

x is the position along the roll thickness (measured from the outer layer) and t is the diffusion time. The pressurization and depressurization times being of a few minutes, the diffusion time t was considered equal to the static impregnation time at the desired T and P conditions [34]. During the impregnation process, the flap of film became saturated and provided the value of carvone concentration in the polymer at the polymer-fluid interface (C_0). Saturation was confirmed by quantifying the carvone concentration in the flap and comparing to the impregnation yield previously obtained at similar conditions.

It has to be noted that Eq. (3) is a valid solution only for semi-infinite slabs, and therefore only experiments where carvone diffusion did not reach the inner layers of the roll were considered for estimating D_{SC} values. These were estimated by fitting Eq. (3) to the experimental concentration profiles using the MS Excel Solver tool, by minimizing the sum of squared errors (*SSE*) calculated according to Eq. (5):

$$SSE = \sum_{i=1}^{NP} \left[\left(\frac{C}{C_0}\right)_{exp} - \left(\frac{C}{C_0}\right)_{calc} \right]^2 \tag{5}$$

where *NP* is the number of experimental and calculated points.

2.8. Release kinetics at ambient conditions

The release kinetics of carvone from impregnated LDPE films into air was determined gravimetrically by monitoring the mass decrease of rectangular film samples of approx. 12 cm^2 exposed to air, at different time intervals until reaching a constant value. These samples were specially impregnated for these tests following the methodology described in Section 2.2, under the same temperature (35 and 60 °C) and CO_2 density (240-700 kg m^{-3}) conditions previously studied. After

impregnation, they were stored in 2 ml hermetic glass vials in refrigerator at 4 °C, until the beginning of the release experiments, in order to minimize the losses of carvone. Release tests were performed at ambient laboratory conditions (20 °C and 1 atm), with air ventilation and controlled relative humidity (approx. 60%). The films were kept in vertical position in order to allow the release from both sides. Neat LDPE films (control) were weighed along with the impregnated samples in order to dismiss any possible weight variation due to ambient humidity absorption or desorption.

The diffusion coefficient values of carvone in LDPE at ambient conditions (D_a) were estimated by fitting a Fickian mass transfer model for non-steady diffusion to the experimental cumulative release curves [40–43], given by Eq. (6):

$$\frac{M_t}{M_\infty} = 1 - \frac{8}{\pi^2}\sum_{n=0}^{\infty}\frac{1}{(2n+1)^2}exp\left[-\frac{(2n+1)^2\pi^2}{L^2}D_a t\right] \quad (6)$$

where M_t is the mass of carvone released after time t, M_∞ is the total released mass (or the initial carvone content in the film) and L is the film thickness. This analytical solution of second Fick's law is valid under the following assumptions: (a) the diffusion process can be described by Fick's laws; (b) the diffusion coefficient is constant during the desorption process (i.e., concentration-independent), which can be assumed when the concentration of solute is low; (c) mass transfer only occurs in the direction of the film thickness (unidimensional diffusion), and edge effects are negligible; (d) the only resistance to mass transfer is located in the polymer side (perfect sink conditions can be assumed in the air side); (e) the initial concentration of carvone in the film is uniform.

This model has been applied by many authors for the mathematical description of absorption/desorption processes into/from polymers, in gas and liquid phase, such as the absorption of flavor compounds (terpenes, esters and phenolics) by food packaging films [44–48] and the emission of volatiles (phenol, dodecane) from polymeric building materials [49]. Eq. (6) involves an infinite series of terms. In our calculations, only the first 20 terms were included, due to the fact that the contribution of the terms for $n > 20$ proved to be negligible. The model fitting was performed using the Microsoft Excel Solver tool, minimizing the sum of squared errors (*SSE*), calculated according to Eq. (7):

$$SSE = \sum_{i=1}^{NP}\left[\left(\frac{M_t}{M_\infty}\right)_{exp} - \left(\frac{M_t}{M_\infty}\right)_{calc}\right]^2 \quad (7)$$

where *NP* is the number of experimental and calculated points

2.9. Statistical analysis

All experiments were performed at least in duplicate. The results were expressed as: mean value ± standard deviation. The differences in mean values between samples were assessed using Student's *t*-test and were considered significant at $p < 0.05$.

3. Results and discussion

3.1. Supercritical impregnation of R-(–)-carvone in polymeric films

As previously mentioned, preliminary calculations of the carvone solubility in CO_2 were performed with the GC-EOS model, in order to select a concentration value to be used in all impregnation experiments. Fig. 4(a) shows the calculated solubility of carvone as a function of pressure at 39 and 49 °C, in comparison with experimental data reported in the literature [38,39]. The numerical values, as well as the model deviation (expressed as AARD%), are provided in Table 2. It can be seen that the GC-EOS predictions reproduced satisfactorily the experimental solubility data, which is a remarkable feature of this model previously assessed with other terpene compounds [50,51]. Therefore, predictive calculations at the selected impregnation temperatures (35 and 60 °C) were performed, as shown in Fig. 4(b). From these data, a fixed mole fraction of carvone in the fluid phase of $y = 2.4 \times 10^{-4}$ (corresponding to 0.8 mg/g CO_2) was selected for all the impregnation experiments. This value corresponded to the lowest concentration of our experimental design, therefore ensuring single phase conditions for the CO_2 phase in all runs.

As described in Section 2.4, the impregnated films were analyzed by FTIR spectroscopy in order to confirm the incorporation of carvone. Absorption spectra of pure carvone, neat LDPE and impregnated LDPE films are shown in Fig. 5. It can be seen that the typical absorbance band of the carbonyl group at $\sim 1680\ cm^{-1}$ is present in the impregnated film spectrum, indicating the incorporation of carvone. In addition, no changes are observed in the LDPE sprectrum that could indicate chemical modification of the polymer due to the impregnation treatment.

The effect of CO_2 density (240-700 kg m^{-3}) at two different temperature levels (35 and 60 °C) on the impregnation yield of LDPE films with carvone was investigated. Results are presented graphically in Fig. 6. As can be seen, impregnation yield ranged from 2.0 to 4.8% (w/w), at both temperatures. These values are in agreement with data previously reported by the authors regarding the impregnation of LDPE with other terpene compounds (eugenol, pulegone, thymoquinone) [7,26], as well as data reported by other authors using LDPE and related compounds such as thymol [28], 2-nonanone [29] and clove essential oil [1]. These relatively low values suggest that LDPE has a limited loading capacity, which can be explained by the combination of several factors: (a) the absence of polar functional groups capable of strong interactions with the solute molecules; (b) the semicrystalline nature of the polymer, with amorphous domains easily impregnable and crystalline regions with very limited sorption capacity; and (c) the high solubility of these types of solutes in $scCO_2$, yielding high partition coefficients between the fluid phase and the polymer.

It can be observed that yield values decrease with $scCO_2$ density. Moreover, this effect seems independent of temperature, as nearly the same trend and values were obtained at 35 and 60 °C. The role of CO_2 density in the impregnation process has been previously observed and discussed. On one hand, CO_2 sorption by the polymer is enhanced at high density conditions, facilitating the diffusion and penetration of solute molecules. On the other hand, the solvent power of $scCO_2$ increases with density, and therefore the partition coefficient is enhanced towards the fluid phase. The interplay of both effects may determine different behaviors. In this sense, an increase [52], a decrease [53] or a maximum yield at an intermediate density value [54,55] have been reported by different authors. The occurrence of each behavior will depend on the particular system studied, as discussed by Champeau et al. [52]. In our case, the decreasing of impregnation yield over the broad density range studied reveals that the effect on the solute partition coefficient is predominant, which seems to be the typical behavior in systems composed by solutes of high solubility and non-polar polymers. Additionally, the fact that temperature has no effect on carvone loading may be the result of two counterbalanced phenomena: an increase of carvone vapor pressure with temperature (which favors its fluid/polymer partition coefficient), and a diffusivity increase (by increasing the molecular motion of both the solute and the polymer chains).

3.2. Thermal and mechanical properties

Thermograms of neat and impregnated LDPE films are presented in Fig. 7. The main melting temperatures and the calculated crystallinity degree are reported in Table 3. The impregnated samples correspond to three different temperature/density conditions: (A) 35 °C/273 kg m^{-3}, (B) 35 °C/700 kg·m^{-3} and (C) 60 °C/272 kg m^{-3}. In the case of neat LDPE, two main melting regions can be observed, identified as T_{m3} and T_{m4}, located at approx. 111 °C and 118 °C, which may be assigned to two populations of crystalline lamellae with different thickness or

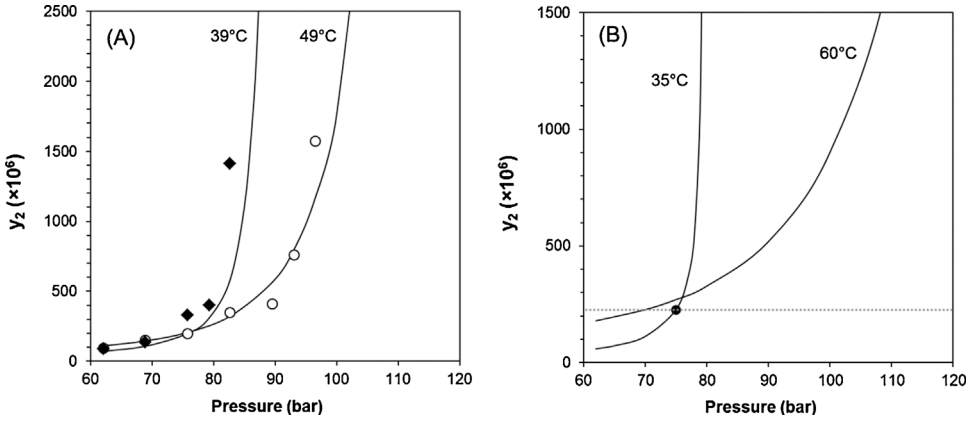

Fig. 4. Solubility of carvone (y_2) in $scCO_2$ as a function of pressure. (A) Dots: experimental values at (♦) T = 39 °C and (○) T = 49 °C [38,39]. Solid lines: GC-EOS predictions. (B) GC-EOS predictions at T = 35 °C and T = 60 °C and selected concentration value.

Table 2
Experimental [38,39] and calculated solubility of carvone in CO_2.

T (°C)	P (MPa)	CO_2 density (kg m^{-3})	$y_{exp} \times 10^6$	$y_{calc} \times 10^6$	AARD%
39	6.21	160.2	90	71	32.8
	6.89	195.0	136	107	
	7.58	244.4	331	198	
	7.93	280.6	400	310	
	8.27	323.2	1411	583	
49	6.21	143.6	92	110	15.0
	6.89	169.5	150	145	
	7.58	200.6	198	206	
	8.27	239.1	349	322	
	8.96	289.4	409	567	
	9.31	321.7	757	801	
	9.65	358.4	1571	1165	

degree of perfection. Besides, a minor peak T_{m1} appears at ~48 °C, indicative of short chain and more defective lamellae. This multiple melting behavior is typical of blends containing different types of LDPE, as is usually the case in the commercial blown films [32,56]. Some modifications can be observed after impregnation. In the samples impregnated at 35 °C, the main feature that can be noticed is that T_{m1} shifts to a higher value (~55 °C). T_{m3} and T_{m4} are not altered, but in the samples impregnated at 700 kg·m^{-3} (B) the T_{m4} peak becomes narrower. These results suggest that CO_2 sorption as well as the incorporation of carvone, had a plasticizing effect that promoted recrystallization phenomena. On one hand, T_{m1} crystals recrystallized forming more perfect and thicker lamellae, with higher melting point, and this phenomenon occurs equally at low and high CO_2 density, suggesting that this effect is independent of the concentration of carvone in the film. In the case of T_{m4} crystals, the narrower peak in sample B may indicate that the morphology of this population becomes more homogeneous. These thicker and more perfect crystals melt at a much higher temperature than the impregnation condition, and therefore a higher CO_2 sorption degree is required for plasticization, which explains the fact that this phenomenon is only appreciated at high CO_2 density conditions.

On the contrary, in the case of sample C (impregnated at 60 °C) T_{m1} is reduced to 42 °C, while a distinct melting region (T_{m2}) appears at 85 °C. Plasticization is expected to increase with temperature, and in this case a crystal population which originally melted in a broad range about 85 °C, recrystallizes in a preferential orientation producing a narrower peak at this specific temperature.

As can be seen in Table 3, the total crystallinity degree of LDPE films is not significantly altered, showing a slight increase which is highest when operating at low temperature and high CO_2 density. Therefore, it could be concluded that the crystalline domains undergo morphological changes and a reorganization process, without the net formation of new crystals. However, further studies by X-ray diffraction analysis should be performed in order to gain deeper insight of these changes in the crystalline phases during the impregnation process.

The effect of $scCO_2$ impregnation process on the mechanical properties of LDPE films is shown in Table 4, where the Young modulus, yield strength, tensile strength and elongation at break (or ductility) are given for neat, $scCO_2$-treated and carvone-loaded LDPE films, obtained at 35 °C and two CO_2 density conditions (~270 and 700 kg m^{-3}). In Fig. 8, some typical strain-stress curves are provided. In Table 4, it can be seen that the tensile strength of the films is not significantly affected by the pure $scCO_2$ treatment itself, but the impregnation with carvone reduces it in approx. 15% compared to the neat film, but only when it is performed under high density conditions. The same trend can be observed with the Young modulus, which is significantly affected only by

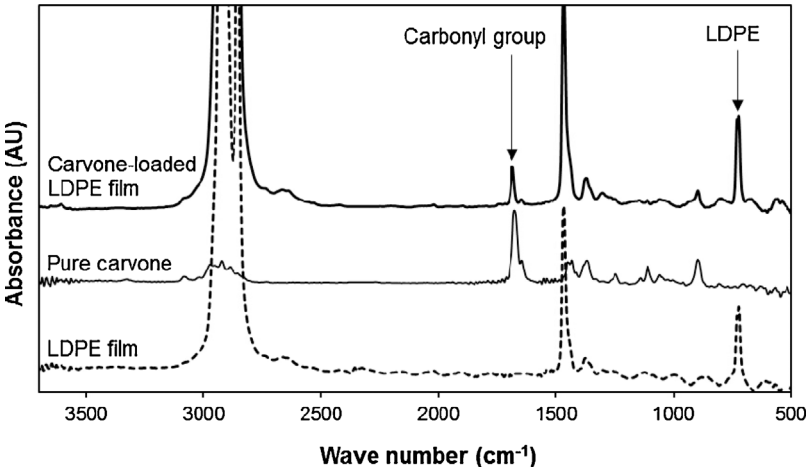

Fig. 5. FT-IR spectra of LDPE film, pure carvone and carvone-loaded LDPE film (impregnation conditions: T = 35 °C, CO_2 density = 240 kg m^{-3}, t = 2 h, depressurization rate = 0.6 MPa min^{-1}). AU: Arbitrary units.

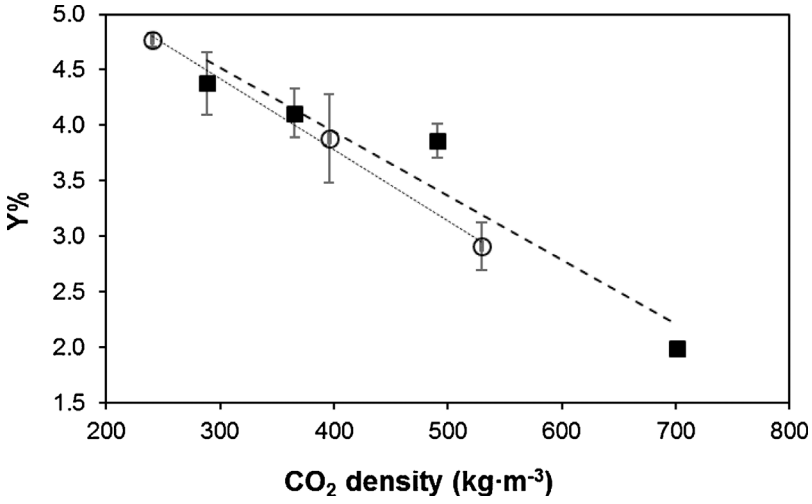

Fig. 6. Effect of process conditions on the impregnation yield (*Y*%) of carvone in LDPE films at T = 35 °C (■) and T = 60 °C (○). Vertical bars represent standard deviation. Lines only provide eye guidance.

impregnation at high density conditions. The yield strength, which represents the starting point of plastic deformation, is reduced by the pure $scCO_2$ treatment itself as well as by the incorporation of carvone at high density conditions. The elongation at break was not significantly affected, but it has to be noted that the deviations among samples were high.

The analysis of these results suggests that neither the incorporation of carvone nor the CO_2 treatment alone explain by themselves the observed trends, which appear as a combination of both factors: on one hand, the plasticizing effect caused by the incorporation of small penetrant molecules, which affect the mobility of polymer chains of the amorphous zones, as previously observed for LDPE films impregnated with other terpene compounds [26]; on the other hand, the above mentioned orientation effect under recrystallization conditions induced by $scCO_2$ sorption, which was stronger under high density conditions, and may further facilitate the mobility of entire polymer regions as reflected in the mechanical behavior changes. As a result of the interplay of both phenomena, the plasticization of this material seems to require the presence of carvone molecules as well as the rearrangements induced by high CO_2 density. The fact that the most significant effects were observed at a condition where the carvone concentration in the films was lower may indicate a "saturation" behavior for this phenomenon. A more systematic correlation between thermal and mechanical analysis data should be required in order to gain deeper insight on this hypothesis.

3.3. Diffusion coefficient estimation under impregnation conditions

The amount of carvone loaded into the cell for the impregnation of film rolls was calculated taking into account the solubility of carvone in $scCO_2$ and the impregnation yield obtained at different operation conditions. An excess amount (960 mg) was used in order to ensure that the concentration of carvone in the fluid phase was constant along the experiments (assumption (d) in Section 2.7). This value was in excess with respect to the solubility limit as well as to the hypothetical quantity necessary for impregnating the entire roll at the saturation value (*Y*%).

Adimensional concentration profiles of carvone along the film roll

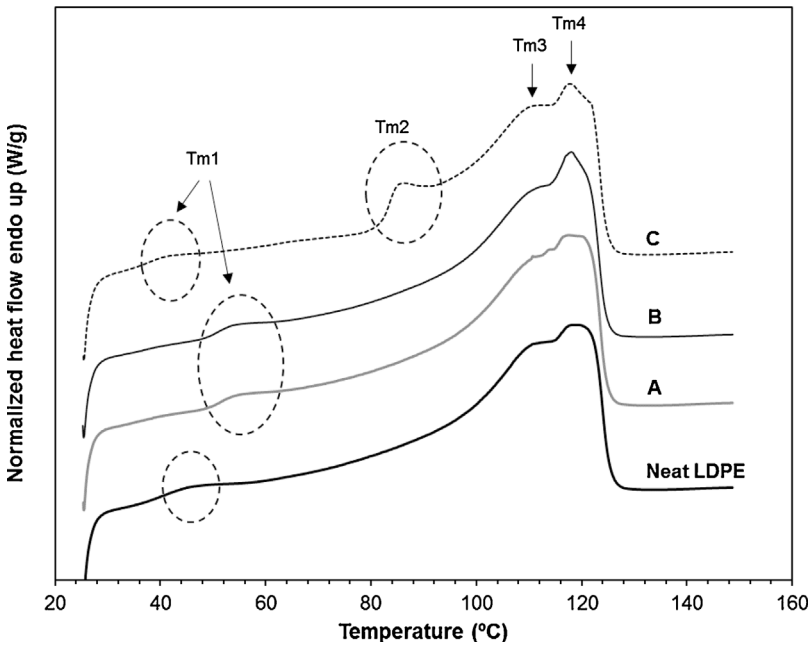

Fig. 7. DSC thermograms for neat and impregnated LDPE films obtained at different process conditions. A: 35 °C-273 kg m^{-3}, B: 35 °C-700 kg m^{-3} and C: 60 °C-272 kg m^{-3}.

Table 3
Thermal properties for neat and impregnated LDPE films, processed at different impregnation conditions (depressurization rate = 0.6 MPa·min^{-1}, time = 2 h).

	T_{imp} (°C)	CO_2 density (kg m^{-3})	T_{m1} (°C)	T_{m2} (°C)	T_{m3} (°C)	T_{m4} (°C)	Crystallinity degree (%)
Neat LDPE	–	–	48	–	111	119	47.60
Carvone-loaded LDPE	35	273	55	–	111	119	49.07
	35	700	55	–	112	118	49.32
	60	700	42	85	110	118	48.43

thickness at different density and temperature conditions are shown in Fig. 9. As explained in Section 2.7, these data were used to estimate diffusion coefficient values for carvone in $scCO_2$-swollen LDPE under impregnation conditions, by fitting Eq. (3). Results are shown in Table 5. It can be seen that D_{SC} increases with temperature as well as with CO_2 density, from 6.5×10^{-11} m^2 s^{-1} (at 35 °C and 273 kg m^{-3}) to 3×10^{-10} m^2·s^{-1} (at 60 °C and 273 kg m^{-3}) and 8.5×10^{-10} m^2 s^{-1} (at 35 °C and 700 kg m^{-3}), respectively. In the first case, it can be assigned to the increased molecular motion of carvone molecules and polymer chains, promoted by temperature. In the case of density, the one-order-of-magnitude increase relies on the free volume increment due to CO_2 absorption and the plasticizing effect of CO_2 molecules, which enhance the mobility of polymer chains, which is in fact the basis for the supercritical impregnation process [9]. Although it is a key factor for designing and modeling CO_2-assisted impregnation processes, there are few works in the literature that report diffusion coefficients in $scCO_2$-swollen polymers, and the available data are mainly related to supercritical dying. Schnitzler and Eggers have reported D_{SC} values of 1.07×10^{-13} m^2/s and 1.93×10^{-11} m^2/s for two synthetic azo dyes (disperse red 324 and dispersed orange 149) in PET samples at 120 °C and 30 MPa (CO_2 density: 585 kg m^{-3}) [57]. Sicardi et al. have reported diffusivity data in the range 1.4×10^{-14}–1.1×10^{-13} m^2/s for disperse blue and disperse yellow in PET films at 90–110 °C and 22–25 MPa (CO_2 density: 484–580 kg m^{-3}), determined by the film roll method [34]. Although the reported values are several orders of magnitude lower than for carvone in LDPE – which is consistent with the higher molecular mass of azo dyes and the different morphology of PET–, these authors have observed the same increase in diffusivity with temperature and CO_2 density.

Diffusion coefficients of similar compounds in LDPE and LLDPE films swollen by (or in contact with) other solvents have been reported in the literature. For example, release kinetics of 2-nonanone [29] and thymol [28] from LLDPE films into food simulants (aqueous solutions of 10–95% ethanol) have been investigated, with diffusion coefficients ranging from 7×10^{-13} to 6×10^{-12} m^2 s^{-1}. Data for linear paraffins in completely swollen LDPE have also been reported, being 1×10^{-12} m^2 s^{-1} for undecane and 9×10^{-13} m^2 s^{-1} for tridecane, measured at 40 °C [58]. Although comparison with other compounds should be done cautiously, these results suggest that diffusivity in $scCO_2$-swollen LDPE is at least one order of magnitude higher than in LDPE swollen with liquid solvents (polar and non-polar) at atmospheric pressure, which is the reason of the shorter contact times required for penetration in $scCO_2$-assisted impregnation and one major advantage of this process.

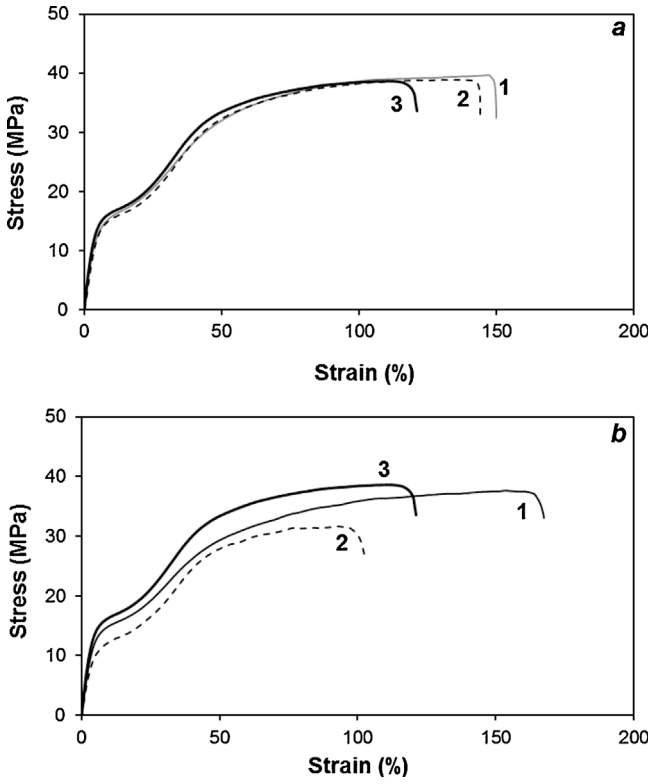

Fig. 8. Stress–strain curves for $scCO_2$-treated LDPE at T = 35 °C and CO_2 density = 273 kg m^{-3} (1) and 700 kg m^{-3} (2), compared with neat LDPE films (3). (a): samples treated only with CO_2 and (b): carvone-impregnated samples.

3.4. Release kinetics at ambient conditions

As previously explained in Section 2.8, the diffusion coefficient of carvone in LDPE films loaded under different impregnation conditions was estimated from the release profiles to air at ambient conditions (D_a). The estimated values are shown in Fig. 10, for all tested conditions. Overall, D_a values range between 3×10^{-14} and 6×10^{-14} m^2 s^{-1}. To the best of our knowledge, there are no data for this particular system in the literature, but results can be compared to

Table 4
Mechanical properties for neat, pressurized and carvone-impregnated LDPE films, at different process conditions (T = 35 °C, depressurization rate = 0.6 MPa·min^{-1}).

	CO_2 density (kg m^{-3})	Young modulus (MPa)	Yield strength (MPa)	Tensile Strength (MPa)	Elongation at break (%)
Neat LDPE	–	345.4 ± 10.7^{a}	14.0 ± 1.2^{a}	38.4 ± 1.9^{a,b,c}	130.6 ± 26.3^{a}
$scCO_2$-treated LDPE	273	330.6 ± 17.4^{a}	12.3 ± 0.5^{b}	39.6 ± 0.8^{a}	151.4 ± 10.3^{a}
	700	328.8 ± 26.5^{a}	12.5 ± 0.6^{b}	38.2 ± 1.1^{a,b,c}	133.1 ± 20.8^{a}
[Carvone + $scCO_2$]-treated LDPE	273	335.7 ± 15.0^{a}	12.3 ± 1.0^{b}	37.3 ± 1.3^{b}	152.6 ± 17.0^{a}
	700	286.3 ± 14.8^{b}	9.8 ± 1.1^{c}	32.8 ± 1.9^{d}	133.2 ± 35.0^{a}

Results are shown as mean values ± standard deviation (n = 6-10).
Different letters in the same column indicate significant differences ($p < 0.05$).

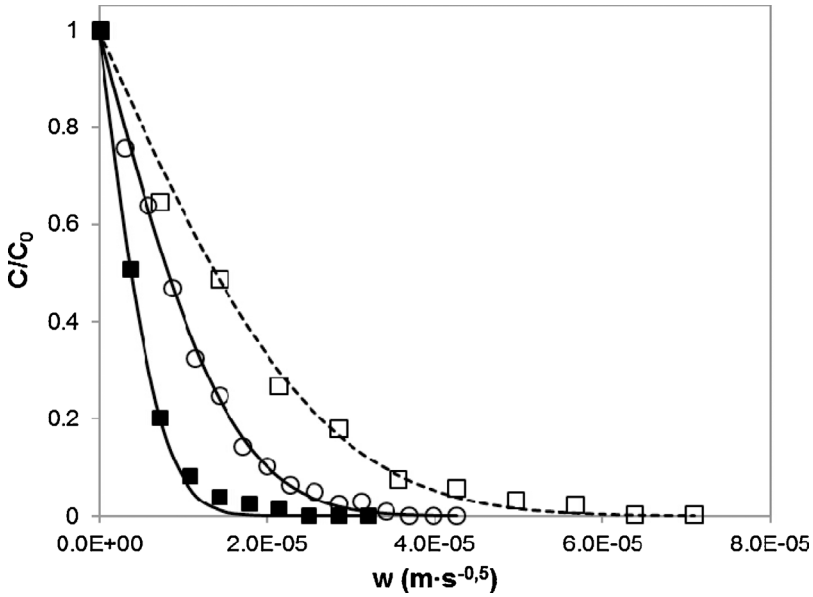

Fig. 9. Penetration curves of *R*-(–)-carvone in LDPE film rolls during supercritical CO_2-assisted impregnation at $T = 35$ °C with low (■, 273 kg m^{-3}) and high (□, 701 kg m^{-3}) CO_2 densities; and $T = 60$ °C with low (○, 272 kg m^{-3}) CO_2 density. Dots: experimental values; solid and dash lines: model fitting.

Table 5
Diffusion coefficient (D_{SC}) for *R*-(–)-carvone in $scCO_2$-swollen LDPE films under impregnation conditions, estimated according to Eq. (3). (t = 2 h, depressurization rate = 0.6 MPa·min^{-1}).

Temperature (°C)	Pressure (MPa)	CO_2 density (kg m^{-3})	$D_{SC} \times 10^{10}$ (m^2 s^{-1})	*NP*	*SSE*
35	7.5	273	0.65	10	0.003
35	9.7	700	8.50	16	0.004
60	9.7	272	3.00	11	0.008

the diffusion coefficient of pulegone −a closely related terpene ketone– in LDPE at 24 °C, which has been reported elsewhere [41] ranging from 1.2×10^{-13} to 4.5×10^{-13} m^2 s^{-1}. The one-order of magnitude observed difference can be attributed to the measurement temperature. Other authors [47] have also reported similar values for the diffusion coefficients of citral (2.5×10^{-13} m^2 s^{-1}) and limonene (1.2×10^{-12} m^2 s^{-1}) at 25 °C, in LDPE. However, as previously mentioned, comparisons with other studies should be performed cautiously, as the density of the LDPE films used by other authors may vary, affecting the diffusivity.

Results indicate that D_a is almost independent of impregnation density at 35 °C, but it increases with impregnation temperature at constant density conditions, especially above ~400 kg m^{-3}. In other words, the combination of $scCO_2$ density and temperature during the impregnation process enhances the observed diffusivity of carvone in the obtained films when released to air at ambient conditions. An explanation can be attempted as follows. Diffusion in semicrystalline polymers is often explained in terms of the network tortuosity, i.e., the path that the solute molecules must follow in order to move across the amorphous regions of the polymer surrounding the impermeable crystalline domains, which act as barriers to diffusion. Therefore, as the crystallinity degree of LDPE is not substantially affected by the treatment (Table 3), diffusion rate will depend on the size, morphology and distribution of the crystallites. It has been reported that the annealing process can reduce the tortuosity factor in semicrystalline polymers up to 50% [59], and this phenomenon has been explained by the formation of semi-permeable gaps or microvoids in the crystallites due to local recrystallization. The absorption of CO_2 under high pressure conditions has been analyzed as analogous to the annealing process, as the increased mobility of polymer chains (CO_2-induced plasticization) allows a similar recrystallization process [60]. Conducting impregnation at higher temperature should enhance this phenomenon. Moreover, it has been shown by DSC analysis that a population of crystals of intermediate melting temperature (T_{m2}) becomes more oriented during recrystallization when impregnation is conducted at 60 °C. As a result of

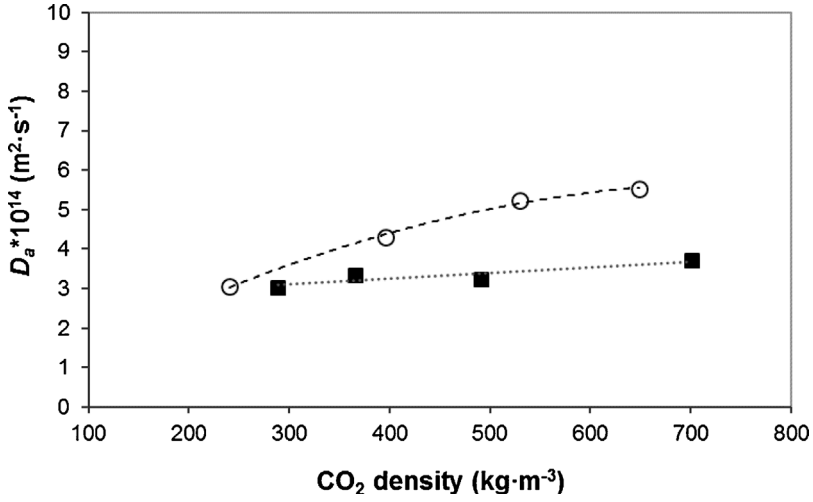

Fig. 10. Effect of impregnation process variables on the diffusion coefficient (D_a) of carvone in LDPE films at room conditions: (■) T_{imp} = 35 °C; (○) T_{imp} = 60 °C. Values estimated by fitting Eq. (6) to experimental measurements (*NP* = 6; *SSE* = 6.0×10^{-4}–1.2×10^{-2}).

all this, the network tortuosity may decrease under these conditions, with a consequent increase in carvone molecules diffusivity, even though the global crystallinity degree does not change. It is also consistent with the increase of the plasticizing effect observed at high CO_2 density previously discussed in the mechanical properties analysis, corresponding to higher mobility and/or free volume of the amorphous zones, which also enhance diffusivity.

4. Conclusions

In this work, the $scCO_2$-assisted impregnation of commercial LDPE films, commonly used as packaging material, with *R*-(–)-carvone –a terpene ketone with antimicrobial and insecticide activity, naturally occurring in many essential oils– was studied. It was observed that the impregnation yield decreases with CO_2 density, showing practically no dependence with temperature at the tested values (35 and 60 °C). This behavior is consistent with the high solubility of this compound in $scCO_2$ and the lack of strong interactions with the polymer. From the point of view of maximizing the amount of active compound in the films while minimizing energetic costs, the best impregnation condition among the operational range studied in this work would be at the lowest temperature and density conditions (35 °C and $\sim$290 kg m^{-3}, corresponding to a pressure of 7.6 MPa), obtaining an impregnation yield (*Y*%) of 4.38 ± 0.28%.

Thermal and mechanical properties of the obtained films showed some degree of plasticization, reflected in lower Young modulus and yield strength values, especially in the samples impregnated with carvone under high CO_2 density conditions.

The diffusion coefficient of carvone in $scCO_2$-swollen LDPE films could be estimated by the film-roll method, being several orders of magnitude higher than the diffusion coefficients in the non-swollen polymer at ambient conditions (10^{-10} vs 10^{-14} m^2 s^{-1}), determined from the release kinetics to air. This information is fundamental for the design and optimization of an impregnation process of film rolls (or pieces with higher thickness) as well as for the modeling of the release process and the prediction of the life time of the packaging material.

In conclusion, the optimal impregnation conditions will depend on the requirements of each specific application, and therefore in the suitable combination of carvone content, mechanical behavior and release profile.

Acknowledgments

The authors gratefully acknowledge the financial support of Consejo Nacional de Investigaciones Científicas y Técnicas (PIP 0941, CONICET, Argentina), Agencia Nacional de Promoción Científica y Tecnológica (StartUp PICT-2011-0726, ANPCYT, Argentina) and Universidad Tecnológica Nacional (PID 3486 and PID 3458, UTN, Argentina). M.L. Goñi thanks CONICET (Argentina) for her postdoctoral fellowship. N.A. Gañan, R.E. Martini and A.E. Andreatta are carrier members of CONICET (Argentina). The authors also thank Dr. Jimena Herrera and Dr. Pablo Ribotta for their technical support.

Appendix A. GC-EOS equations and parameters for the calculation of carvone solubility in $scCO_2$

As mentioned in Section 2.3, the solubility of carvone in $scCO_2$ was modeled using the Group Contribution Equation of State (GC-EOS). The detailed description of this model can be found in the works by Skjold-Jørgensen [36]. Briefly, the GC-EOS model computes the residual Helmholtz energy (A^{res}) by two additive contributions: a repulsive or free volume term (A^{fv}) and an attractive term accounting for intermolecular forces (A^{att}):

$$A^{res} = A^{fv} + A^{att} \tag{A1}$$

The free volume term is modeled using a Carnahan-Starling type hard sphere expression, developed by Mansoori and Leland [61]:

$$\frac{A^{fv}}{RT} = 3\left(\frac{\lambda_1\lambda_2}{\lambda_3}\right)(Y-1) + \left(\frac{\lambda_2^3}{\lambda_3^2}\right)(-Y + Y^2 - \ln Y) + n\ln Y \tag{A2}$$

where:

$$Y = \left(1 - \frac{\pi\lambda_3}{6V}\right)^{-1} \tag{A3}$$

$$\lambda_k = \sum_i^{NC} n_i d_i^k \tag{A4}$$

V is the total volume, NC the number of components in the mixture, n_i is the number of moles of component i, n is the total mole number and d_i is the temperature dependent hard sphere diameter of each component, calculated as:

$$d_i = 1.065655 d_{ci}\left[1 - 0.12\exp\left(\frac{-2T_{ci}}{3T}\right)\right] \tag{A5}$$

where d_{ci} is the pure component critical hard sphere diameter. This parameter can be fitted to a vapor pressure point, or calculated from the pure compound critical properties (T_c and P_c) as:

$$d_{ci} = \left(\frac{0.08943 RT_{ci}}{P_{ci}}\right)^{1/3} \tag{A6}$$

The attractive term is a group contribution version of a NRTL type expression [62] with density dependent mixing rules:

$$\frac{A^{att}}{RT} = -\frac{z}{2}\sum_i^{NC} n_i \sum_j^{NG} \nu_j^i q_j \sum_k^{NG} (\theta_k g_{kj}\tilde{q}\tau_{kj}/RTV)/\sum_l^{NG} \theta_l \tau_{lj} \tag{A7}$$

where:

$$\theta_j = \left(\frac{q_j}{\tilde{q}}\right)\sum_i^{NC} n_i \nu_j^i \tag{A8}$$

Table A1
Pure compounds physicochemical properties.

	M_W (g mol^{-1})	T_c (K)	P_c (MPa)	T_{sat} (K)	P_{sat} (MPa)
CO_2	44.0	304.2	7.28	–	–
Carvone	150.2	724.5[a]	2.82[a]	355.2[b]	0.00053[b]

[a] Estimated by Joback group contribution method [66].
[b] Data from literature [67].

Table A2
Group structure of pure compounds.

Group	CO_2	Carvone
CH_3	–	2
$cyCH_2$	–	1
cyCH	–	1
$C{=}CH_2$	–	1
C=CH	–	1
$CH_2C{=}O$	–	1
CO_2	1	–

Table A3
GC-EOS pure group parameters.

Group	T^*	q	g	g'	g''
CH_3	600.0	0.848	316910	−0.9274	0
$cyCH_2$	600.0	0.540	466550	−0.6062	0
cyCH	600.0	0.228	466550	−0.6062	0
$C{=}CH_2$	600.0	0.988	323400	−0.6328	0
C=CH	600.0	0.676	546780	−1.0966	0
$CH_2C{=}O$	600.0	1.180	888410	−0.7018	0
CO_2	304.2	1.261	531890	−0.5780	0

Table A4
Binary interaction parameters (k_{ij} above diagonal, k'_{ij} below diagonal).

Group	CH_3	$cyCH_2$	cyCH	$C{=}CH_2$	C=CH	$CH_2C{=}O$	CO_2
CH_3	1	1	1	1	0.977	0.834	0.898
$cyCH_2$	0	1	1	1.040	1	0.870	0.928
cyCH	0	0	1	1.040	1	0.870	0.928
$C{=}CH_2$	0	0	0	1	1.094	1	1.057
C=CH	0	0	0	0	1	0.975	1
$CH_2C{=}O$	0.084	0.097	0.097	0	0	1	1.025
CO_2	0	0.210	0.210	0	0	0.108	1

$$\tilde{q} = \sum_{i}^{NC} n_i \sum_{j}^{NG} \nu_j^i q_j \tag{A9}$$

$$\tau_{ij} = \exp\left(\frac{\alpha_{ij}\Delta g_{ij}\tilde{q}}{RTV}\right) \tag{A10}$$

$$\Delta g_{ij} = g_{ij} - g_{jj} \tag{A11}$$

NG is the number of groups, z is the coordination number of any segment (set to 10), ν_j^i is the number of groups of type j in molecule i, q_j is the number of surface segments assigned to group j, θ_k is the surface fraction of group k, $\tilde{q}$ is the total number of surface segments, g_{ij} is the attraction energy parameter between groups i and j ($g_{ij} = g_{ji}$), and α_{ij} is the binary non-randomness parameter ($\alpha_{ij} \neq \alpha_{ji}$). The binary interaction parameters between unlike groups are calculated as:

$$g_{ij} = k_{ij}(g_{ii}g_{jj})^{1/2}(k_{ij} = k_{ji}) \tag{A12}$$

with the following temperature dependences:

$$g_{jj} = g_{jj}^*\left[1 + g_{jj}^{'}\left(\frac{T}{T_j^*} - 1\right) + g_{jj}^{''}\ln\left(\frac{T}{T_j^*}\right)\right] \tag{A13}$$

Table A5
Binary non-randomness parameters (a_{ij} above diagonal, a_{ji} below diagonal).

Group	CH_3	$cyCH_2$	cyCH	$C{=}CH_2$	C=CH	$CH_2C{=}O$	CO_2
CH_3	0	0	0	0	0	0.854	4.683
$cyCH_2$	0	0	0	0	0	0.854	0
cyCH	0	0	0	0	0	0.854	0
$C{=}CH_2$	0	0	0	0	0	0	0
C=CH	0	0	0	0	0	0	0
$CH_2C{=}O$	5.146	5.146	5.146	0	0	0	0.170
CO_2	4.683	0	0	0	0	0.170	0

$$k_{ij} = k_{ij}^{*}\left[1 + k_{ij}^{'}\ln\left(\frac{2T}{T_i^{*} + T_j^{*}}\right)\right] \tag{A14}$$

where g_{jj}^{*} is the interaction parameter for the pure group j at the reference temperature T_j^{*}.

The relevant physico-chemical properties of carvone and CO_2 are presented in Table A1. The GC-EOS group structures are presented in Table A2. The pure group, binary interaction and binary non-randomness parameters used in the model are reported in Tables A3–A5 and correspond to the latest updates available in the literature [51,63–65].

References

[1] G.R. Medeiros, S.R.S. Ferreira, B.A.M. Carciofi, High pressure carbon dioxide for impregnation of clove essential oil in LLDPE films, Innov. Food Sci. Emerg. Technol. 41 (2017) 206–215, http://dx.doi.org/10.1016/j.ifset.2017.03.008.

[2] C.C. Bastante, L.C. Cardoso, C.M. Serrano, E.J.M. De Ossa, Supercritical impregnation of food packaging films to provide antioxidant properties, J. Supercrit. Fluids 128 (2017) 200–207, http://dx.doi.org/10.1016/j.supflu.2017.05.034.

[3] A. Torres, E. Ilabaca, A. Rojas, F. Rodríguez, M.J. Galotto, A. Guarda, C. Villegas, J. Romero, Effect of processing conditions on the physical, chemical and transport properties of polylactic acid films containing thymol incorporated by supercritical impregnation, Eur. Polym. J. 89 (2017) 195–210, http://dx.doi.org/10.1016/j.eurpolymj.2017.01.019.

[4] C. Villegas, A. Torres, M. Rios, A. Rojas, J. Romero, C.L. de Dicastillo, X. Valenzuela, M.J. Galotto, A. Guarda, Supercritical impregnation of cinnamaldehyde into polylactic acid as a route to develop antibacterial food packaging materials, Food Res. Int. (2017) 0–1, http://dx.doi.org/10.1016/j.foodres.2017.06.031.

[5] D. Markovic, S. Milovanovic, M. Radetic, B. Jokic, I. Zizovic, Impregnation of corona modified polypropylene non-woven material with thymol in supercritical carbon dioxide for antimicrobial application, J. Supercrit. Fluids 101 (2015) 215–221, http://dx.doi.org/10.1016/j.supflu.2015.03.022.

[6] J.M. Herrera, M.L. Goñi, N.A. Gañán, J.A. Zygadlo, An insecticide formulation of terpene ketones against Sitophilus zeamais and its incorporation into low density polyethylene films, Crop Prot. 98 (2017) 33–39, http://dx.doi.org/10.1016/j.cropro.2017.03.008.

[7] M.L. Goñi, N.A. Gañán, J.M. Herrera, M.C. Strumia, A.E. Andreatta, R.E. Martini, Supercritical CO2 iof LDPE films with terpene ketones as biopesticides against corn weevil (Sitophilus zeamais), J. Supercrit. Fluids 122 (2017) 18–26, http://dx.doi.org/10.1016/j.supflu.2016.11.017.

[8] M.L. Goñi, N.A. Gañán, S.E. Barbosa, M.C. Strumia, R.E. Martini, Supercritical CO2-assisted impregnation of LDPE/sepiolite nanocomposite films with insecticidal terpene ketones: impregnation yield, crystallinity and mechanical properties assessment, J. Supercrit. Fluids 130 (2017) 337–346, http://dx.doi.org/10.1016/j.supflu.2017.06.013.

[9] S.G. Kazarian, Polymer processing with supercritical fluids, Polym. Sci. 42 (2000) 78–101, http://dx.doi.org/10.1080/03602549909351647.

[10] E. Kiran, Supercritical fluids and polymers −The year in review −2014, J. Supercrit. Fluids 110 (2016) 126–153, http://dx.doi.org/10.1016/j.supflu.2015.11.011.

[11] I. Kikic, F. Vecchione, Supercritical impregnation of polymers, Curr. Opin. Solid State Mater. Sci. 7 (2003) 399–405, http://dx.doi.org/10.1016/j.cossms.2003.09.001.

[12] D.L. Tomasko, H.B. Li, D.H. Liu, X.M. Han, M.J. Wingert, L.J. Lee, K.W. Koelling, A review of CO(2) applications in the processing of polymers, Ind. Eng. Chem. Res. 42 (2003) 6431–6456, http://dx.doi.org/10.1021/Ie030199z.

[13] D. Dainelli, Global Legislation for Active and Intelligent Packaging Materials, Elsevier Ltd., 2015, 2017, http://dx.doi.org/10.1016/B978-1-78242-014-9.00008-5.

[14] European Commission, Commission Regulation (EC) No. 450/2009 of 29 May 2009 on Active and Intelligent Materials and Articles Intended to Come into Contact with Food, (2009).

[15] J. Barros-Velasquez, Antimicrobial Food Packaging, Elsevier Inc., San Diego, 2016, http://dx.doi.org/10.1017/CBO9781107415324.004.

[16] C. Morcia, G. Tumino, R. Ghizzoni, V. Terzi, Carvone (Mentha spicata L.) oils, in: R. Victor Preedy (Ed.), Essent. Oils Food Preserv. Flavor Saf. Elsevier Inc., Amsterdam, 2015, pp. 309–316, , http://dx.doi.org/10.1016/B978-0-12-416641-7.00035-3.

[17] S. Burt, Essential oils: their antibacterial properties and potential applications in foods–a review, Int. J. Food Microbiol. 94 (2004) 223–253, http://dx.doi.org/10.1016/j.ijfoodmicro.2004.03.022.

[18] M. Lacroix, The use of essential oils and bacteriocins as natural antimicrobial and antioxidant compounds, Food 1 (2007) 181–192.

[19] P.A. Eliopoulos, C.N. Hassiotis, S.S. Andreadis, A.E.E. Porichi, Fumigant toxicity of essential oils from basil and spearmint against two major pyralid pests of stored products, J. Econ. Entomol. 108 (2015) 805–810, http://dx.doi.org/10.1093/jee/tov029.

[20] J.M. Herrera, M.P. Zunino, Y. Massuh, R. Pizzollito, S. Dambolena, N.A. Gañan, J.A. Zygadlo, Fumigant toxicity of five essential oil rich in ketones against Sitophilus zeamais (Motschulsky), AgriScientia 31 (2014) 35–41 http://www.agriscientia.unc.edu.ar/volumenes/pdf/v31n01a04.pdf.

[21] M.D. López, M.J. Pascual-Villalobos, Insecticidal activity of volatile monoterpenoids to sitophilus oryzae L. (Coleoptera: curculionidae), rhyzopertha dominica fabricius (Coleoptera: bostrichidae) and cryptolestes pusillus schönherr (Coleoptera: cucujidae), in: S. Navarro, C. Adler, L. Stengård Hansen (Eds.), Integr. Prot. Stored Prod., Poznan, 2008, pp. 211–219 http://citeseerx.ist.psu.edu/viewdoc/download?doi=10.1.1.426.4777&rep=rep1&type=pdf#page=62.

[22] A.K. Tripathi, V. Prajapati, S. Kumar, Bioactivities of l-Carvone, d-Carvone, and dihydrocarvone toward three stored product beetles, J. Econ. Entomol. 96 (2003) 1594–1601, http://dx.doi.org/10.1603/0022-0493-96.5.1594.

[23] F. Sadaka, C. Nguimjeu, C.H. Brachais, I. Vroman, L. Tighzert, J.P. Couvercelle, Review on antimicrobial packaging containing essential oils and their active biomolecules, Innov. Food Sci. Emerg. Technol. (2014), http://dx.doi.org/10.1016/j.ifset.2014.03.002.

[24] M. Ramos, A. Jiménez, M. Peltzer, M.C. Garrigós, Characterization and antimicrobial activity studies of polypropylene films with carvacrol and thymol for active packaging, J. Food Eng. 109 (2012) 513–519, http://dx.doi.org/10.1016/j.jfoodeng.2011.10.031.

[25] P. Suppakul, J. Miltz, K. Sonneveld, S.W. Bigger, Characterization of antimicrobial films containing basil extracts, Packag. Technol. Sci. 19 (2006) 259–268, http://dx.doi.org/10.1002/pts.729.

[26] M.L. Goñi, N.A. Gañán, M.C. Strumia, R.E. Martini, Eugenol-loaded LLDPE films with antioxidant activity by supercritical carbon dioxide impregnation, J. Supercrit. Fluids 111 (2016) 28–35, http://dx.doi.org/10.1016/j.supflu.2016.01.012.

[27] M. Mulla, J. Ahmed, H. Al-Attar, E. Castro-Aguirre, Y.A. Arfat, R. Auras, Antimicrobial efficacy of clove essential oil infused into chemically modified LLDPE film for chicken meat packaging, Food Control 73 (2017) 663–671, http://dx.doi.org/10.1016/j.foodcont.2016.09.018.

[28] A. Torres, J. Romero, A. Macan, A. Guarda, M.J. Galotto, Near critical and supercritical impregnation and kinetic release of thymol in LLDPE films used for food packaging, J. Supercrit. Fluids 85 (2014) 41–48, http://dx.doi.org/10.1016/j.supflu.2013.10.011.

[29] A. Rojas, D. Cerro, A. Torres, M.J. Galotto, A. Guarda, J. Romero, Supercritical impregnation and kinetic release of 2-nonanone in LLDPE films used for active food packaging, J. Supercrit. Fluids 104 (2015) 76–84, http://dx.doi.org/10.1016/j.supflu.2013.10.011.

[30] M. Banchero, Supercritical fluid dyeing of synthetic and natural textiles −a review, Color. Technol. 129 (2013) 2–17.

[31] H. Zheng, J. Zhang, J. Yan, L. Zheng, An industrial scale multiple supercritical carbon dioxide apparatus and its eco-friendly dyeing production, J. CO2 Util. 16 (2016) 272–281, http://dx.doi.org/10.1016/j.jcou.2016.08.002.

[32] J. Lu, H.-J. Sue, Morphology and mechanical properties of blown films of a low-density polyethylene/linear low-density polyethylene blend, J. Polym. Sci. Part B Polym. Phys. 40 (2002) 507–518, http://dx.doi.org/10.1002/polb.10115.

[33] Y.-T. Shieh, J.-H. Su, G. Manivannan, P.H.C. Lee, S.P. Sawan, W.D. Spall, Interaction of supercritical carbon dioxide with polymers I. Crystalline polymers, J. Appl. Polym. Sci. 59 (1996) 695–705.

[34] S. Sicardi, L. Manna, M. Banchero, Diffusion of disperse dyes in PET films during impregnation with a supercritical fluid, J. Supercrit. Fluids 17 (2000) 187–194, http://dx.doi.org/10.1016/S0896-8446(99)00055-8.
[35] NIST Chemistry Webbook, (2017) (accessed May 2, 2017), http://webbook.nist.gov/chemistry/fluid/.
[36] S. Skjold-Jørgensen, Group contribution equation of state (GC-EOS): a predictive method for phase equilibrium computations over wide ranges of temperature and pressures up to 30 MPa, Ind. Eng. Chem. Res. 27 (1988) 110–118, http://dx.doi.org/10.1021/ie00073a021.
[37] M.L. Michelsen, The isothermal flash problemPart II. Phase-split calculation, Fluid Phase Equilib. 9 (1982) 21–40, http://dx.doi.org/10.1016/0378-3812(82)85002-4.
[38] K.H. Kim, J. Hong, Equilibrium solubilities of spearmint oil components in supercritical carbon dioxide, Fluid Phase Equilib. 164 (1999) 107–115, http://dx.doi.org/10.1016/S0378-3812(99)00248-4.
[39] R.B. Gupta, J.-J. Shim, Solubility in Supercritical Carbon Dioxide, CRC Press, Boca Raton, 2007.
[40] J. Crank, The Mathematics of Diffusion, 2nd ed., (1975), http://dx.doi.org/10.1016/0306-4549(77)90072-X (London).
[41] M.L. Goñi, N.A. Gañan, R.E. Martini, M.C. Strumia, Mass transfer kinetics and diffusion coefficient estimation of bioinsecticide terpene ketones in LDPE films obtained by supercritical CO2-assisted impregnation, J. Appl. Polym. Sci. 134 (2017) 45558, http://dx.doi.org/10.1002/app.20171183.
[42] J. Siepmann, R.A. Siegel, F. Siepmann, Diffusion controlled drug delivery systems, in: J. Siepmann, R.A. Siegel, M. Rathbone (Eds.), Fundam. Appl. Control. Release Drug Deliv. Springer, New York – Dordrecht – Heidelberg– London, 2012, pp. 127–152.
[43] E.L. Cussler, Multicomponent Diffusion, Elsevier Scientific Publishing Company, Amsterdam, 1976.
[44] L. Safa, B. Abbes, Experimental and numerical study of sorption/diffusion of esters into polypropylene packaging films, Packag. Technol. Sci. 15 (2002) 55–64, http://dx.doi.org/10.1002/pts.568.
[45] D. Cava, J.M. Lagarón, A. López-Rubio, R. Catalá, R. Gavara, On the applicability of FT-IR spectroscopy to test aroma transport properties in polymer films, Polym. Test 23 (2004) 551–557, http://dx.doi.org/10.1016/j.polymertesting.2003.11.003.
[46] D. Cava, R. Catala, R. Gavara, J.M. Lagaron, Testing limonene diffusion through food contact polyethylene by FT-IR spectroscopy: film thickness, permeant concentration and outer medium effects, Polym. Test 24 (2005) 483–489, http://dx.doi.org/10.1016/j.polymertesting.2004.12.003.
[47] G.D. Sadler, R.J. Braddock, Absorption of citrus flavor volatiles by low density polyethylene, J. Food Sci. 56 (1991) 35–37, http://dx.doi.org/10.1111/j.1365-2621.1991.tb07969.x.
[48] A. Peychès-Bach, M. Moutounet, S. Peyron, P. Chalier, Factors determining the transport coefficients of aroma compounds through polyethylene films, J. Food Eng. 95 (2009) 45–53, http://dx.doi.org/10.1016/j.jfoodeng.2009.04.012.
[49] S.S. Cox, D. Zhao, J.C. Little, Measuring partition and diffusion coefficients for volatile organic compounds in vinyl flooring, Atmos. Environ. 35 (2001) 3823–3830.
[50] N.A. Gañán, J.S. Dambolena, R.E. Martini, S.B. Bottini, Supercritical carbon dioxide fractionation of peppermint oil with low menthol content − Experimental study and simulation analysis for the recovery of piperitenone, J. Supercrit. Fluids 98 (2015) 1–11, http://dx.doi.org/10.1016/j.supflu.2014.12.018.
[51] N. Gañán, E.A. Brignole, Fractionation of essential oils with biocidal activity using supercritical CO2—Experiments and modeling, J. Supercrit. Fluids 58 (2011) 58–67, http://dx.doi.org/10.1016/j.supflu.2011.04.010.
[52] M. Champeau, J.-M. Thomassin, T. Tassaing, C. Jerome, Drug loading of sutures by supercritical CO2 impregnation: effect of Polymer/Drug interactions and thermal transitions, Macromol. Mater. Eng. 300 (2015) 596–610, http://dx.doi.org/10.1002/mame.201400369.
[53] Y.A. Hussain, C.S. Grant, Ibuprofen impregnation into submicron polymeric films in supercritical carbon dioxide, J. Supercrit. Fluids 71 (2012) 127–135, http://dx.doi.org/10.1016/j.supflu.2012.07.014.
[54] D. Li, B. Han, Impregnation of polyethylene (PE) with styrene using supercritical CO2 as the swelling agent and preparation of PE/Polystyrene composites, Ind. Eng. Chem. Res. 39 (2000) 4506–4509, http://dx.doi.org/10.1021/ie000228v.
[55] Z. Shen, G.S. Huvard, C.S. Warriner, M. Mc Hugh, J.L. Banyasz, M.K. Mishra, CO2-assisted fiber impregnation, Polymer (Guildf). 49 (2008) 1579–1586, http://dx.doi.org/10.1016/j.polymer.2008.01.020.
[56] A. Prasad, A quantitative analysis of low density polyethylene and linear low density polyethylene blends by differential scanning calorimetery and fourier transform infrared spectroscopy methods, Polym. Eng. Sci. 38 (1998) 1716–1728, http://dx.doi.org/10.1002/pen.10342.
[57] J. von Schnitzler, R. Eggers, Mass transfer in polymers in a supercritical CO2-atmosphere, J. Supercrit. Fluids 16 (1999) 81–92, http://dx.doi.org/10.1016/S0896-8446(99)00020-0.
[58] A. Reynier, P. Dole, A. Feigenbaum, Additive diffusion coefficients in polyolefins. II. Effect of swelling and temperature on the D = f(M) correlation, J. Appl. Polym. Sci. 82 (2001) 2434–2443, http://dx.doi.org/10.1002/app.2094.
[59] W. Vieth, W.F. Wuerth, Transport properties and their correlation with the morphology of thermally conditioned polypropylene, J. Appl. Polym. Sci. 13 (1969) 685–712, http://dx.doi.org/10.1002/app.1969.070130410.
[60] K. Mizoguchi, T. Hirose, Y. Naito, CO2-induced crystallization of poly (ethylene terephthalate), Polymer (Guildf). 28 (1987) 1298–1302, http://dx.doi.org/10.1016/0032-3861(87)90441-1.
[61] G.A. Mansoori, T.W.J. Leland, Statistical thermodynamics of mixtures. A new version for the theory of conformal solution, J. Chem. Soc., Faraday Trans. 2 (68) (1972) 320–344.
[62] H. Renon, J.M. Prausnitz, Local compositions in thermodynamic excess functions for liquid mixtures, AIChE J. 14 (1968) 135–144, http://dx.doi.org/10.1002/aic.690140124.
[63] S. Diaz, S. Espinosa, E.A. Brignole, Citrus peel oil deterpenation with supercritical fluids: optimal process and solvent cycle design, J. Supercrit. Fluids. 35 (2005) 49–61, http://dx.doi.org/10.1016/j.supflu.2004.12.002.
[64] T. Fornari, Revision and summary of the group contribution equation of state parameter table: application to edible oil constituents, Fluid Phase Equilib. 262 (2007) 187–209, http://dx.doi.org/10.1016/j.fluid.2007.09.007.
[65] S. Espinosa, T. Fornari, S.B. Bottini, E.A. Brignole, Phase equilibria in mixtures of fatty oils and derivatives with near critical fluids using the GC-EOS model, J. Supercrit. Fluids 23 (2002) 91–102, http://dx.doi.org/10.1016/S0896-8446(02)00025-6.
[66] B.E. Poling, J.M. Prausnitz, J.P. O'Connell, The Properties of Gases and Liquids, 5th ed., McGraw-Hill, New York, 2001.
[67] E. Guenther, The Essential Oils, 3rd, D. Van Nostrand Company, New York, 1957.